

Molecular Physics



An International Journal at the Interface Between Chemistry and Physics

ISSN: (Print) (Online) Journal homepage: https://www.tandfonline.com/loi/tmph20

Benchmark calculations of the ³D Rydberg spectrum of beryllium

Monika Stanke & Ludwik Adamowicz

To cite this article: Monika Stanke & Ludwik Adamowicz (2022): Benchmark calculations of the ³*D* Rydberg spectrum of beryllium, Molecular Physics, DOI: <u>10.1080/00268976.2022.2073281</u>

To link to this article: https://doi.org/10.1080/00268976.2022.2073281





L. WOLNIEWICZ SPECIAL ISSUE



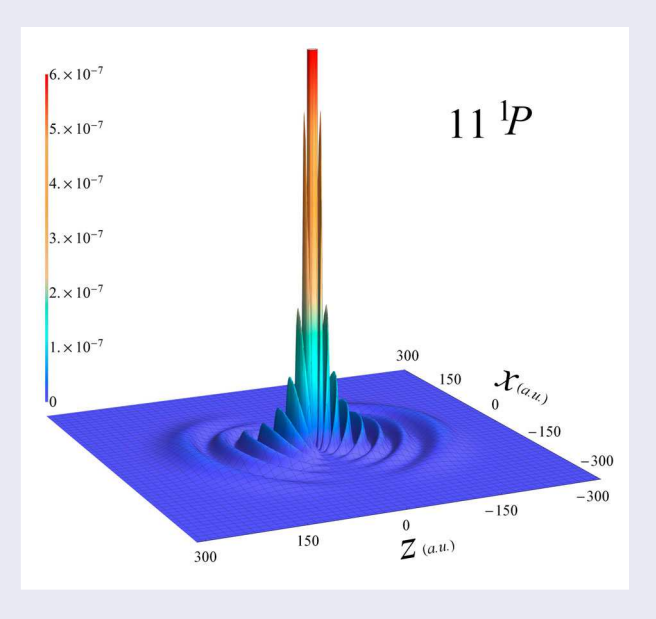
Benchmark calculations of the ³D Rydberg spectrum of beryllium

Monika Stanke^a and Ludwik Adamowicz^{b,c}

^aInstitute of Physics, Faculty of Physics, Astronomy, and Informatics, Nicolaus Copernicus University, Toruń, Poland; ^bDepartment of Chemistry and Biochemistry and Department of Physics, University of Arizona, Tucson, AZ, USA; ^cCentre for Advanced Study (CAS), The Norwegian Academy of Science and Letters, Oslo, Norway

ABSTRACT

High-accuracy calculations are performed for the four lowest 3D states of the beryllium atom. All-electron explicitly correlated Gaussian (ECG) functions are employed to expand the functions and the non-relativistic internal Hamiltonian used in the calculations, which is obtained by rigorously separating out the centre-of-mass motion from the laboratory-frame Hamiltonian, explicitly depends on the finite nuclear mass of 9Be . The nonrelativistic wave functions of the considered states of 9Be are generated variationally with the nonlinear parameters of the Gaussians optimised using a procedure that employs the energy gradient determined with respect to these parameters. The nonrelativistic wave functions are used to calculate the leading relativistic corrections employing the perturbation theory at the first-order level. Only corrections that do not produce fine/hyperfine splitting of the energy levels are considered. The corrections are added to the nonrelativistic energies and the results are used to calculate the so-called 'centre of gravity' transition energies with respect to the 9Be 1S ground state. A comparison with high-quality experimental results shows agreement to within about 0.6 cm $^{-1}$.



ARTICLE HISTORY

Received 25 January 2022 Accepted 26 April 2022

(FYWORDS

High-precision calculations for few-electron (or few-body) atomic systems; relativistic corrections; electron correlation calculations for atoms and ions: excited states; variational techniques; explicitly correlated method

1. Introduction

In this work, we continue our studies of the spectrum of the beryllium atom. The states which are considered are the lowest ³D Rydberg states. As precision spectroscopy of the light elements is quickly advancing, the need to refine the high-accuracy quantum-mechanical

calculations has been an important direction of the theoretical research. The spectrum of the beryllium atom has been expensively studied using the state-of-the-art high resolution spectroscopy methods and has been frequently used to validate the new theoretical models used in atomic calculations [1]. As the neutral four-electron beryllium atom is a relatively simple system, it is usually possible to achieve in the calculations an adequate level of convergence of the results in terms of the number of basis functions provided that the type of functions used in the calculations are capable of very accurately describing the electron correlation effects and have sufficient flexibility to be adjusted to describe individual states. Such flexibility is usually due to the basis functions containing adjustable linear and non-linear parameters that can be variationally optimised in the calculation. In our atomic calculations, we have employed allelectron explicitly correlated Gaussian functions (ECGs). The variational optimisation of the Gaussian exponential parameters performed by the minimisation of the nonrelativistic energy of the considered state of the atom has been key to achieving high accuracy in our atomic ECG calculations (see, e.g., Ref. [1]). The optimisation has involved the use of the analytically determined energy gradient calculated with respect to the Gaussian parameters. Due to the use of the gradient, the basis sets used in our calculations could have been extended to include a large number of ECGs [2-5].

High accuracy atomic calculations also require an accurate account of the leading relativistic and quantum electrodynamics (QED) corrections, as well as the corrections due to the finite mass of the nucleus [6-9]. In our calculations, the account for the effects of the finite nuclear mass is not done is the standard way by employing the perturbation-theory approach, but involves the use in the nonrelativistic variational calculations of a total nonrelativistic Hamiltonian representing the internal state of the system that explicitly depends of the nuclear mass. That Hamiltonian is obtained by separating out the centre-of-mass motion from the laboratoryframe Hamiltonian. The procedure involves transforming the lab-frame Hamiltonian expressed in terms of Cartesian coordinates to a new coordinate system whose first three coordinates are the lab-frame coordinates of the centre of mass and the remaining 3n-3 coordinates are internal coordinates. Some more details about the approach used in our atomic calculations are described in the next section.

We have studied the Rydberg D states of the beryllium atom before using ECGs. First we reported results of nonrelativistic calculations carried out for some lowest 1D states [10]. As those calculations did not include the relativistic corrections, the results disagree with the experimental values by more than the uncertainties of the experimental results. In recent calculations [11], we considered the lowest nine 1D states and the inclusion of the leading spin-independent relativistic energy corrections significantly improved the agreement with the experimental results. In the present work, the

calculations involving the relativistic spin-independent corrections are extended to four lowest 3D states of beryllium.

Measurements of the interstate transitions energies of the beryllium atom have been performed in several works over the last half century. Bozman et al. [12] and Johansson [13] measured an array of the beryllium transitions with $0.01-0.02~{\rm cm}^{-1}$ precision. The measurements performed by Johansson included a transition involving the lowest 1D state, i.e. the $2s2p~^1P \rightarrow 2s3d~^1D$ transition. Measurements of the transitions involving the lowest 1D beryllium states were also reported by Kramida and Martin [14,15].

Even though, ECGs do not strictly satisfy the Kato cusp conditions concerning the behaviour of the electronic wave function at the two-electron coalescent point, if a large number of ECGs are used in expanding the wave function and their parameters are thoroughly optimised in the calculation, the deficiency associated with not satisfying the Kato conditions can be effectively remediated. Besides the explicit dependence of the correlated Gaussian on the inter-electron distances which, as mentioned, is crucial in describing the inter-electron correlation effects, the other main advantage is that the algorithms for calculating for the Hamiltonian and overlap matrix elements, as well as the matrix elements of the energy gradient, with these functions are relatively simple and can be coded into a computer programme in a general form for an arbitrary number of electrons [16]. Also, the ECGs for expanding the wave functions of states with non-zero angular momentum quantum numbers, L, including the D states with L=2 and $M_L=0$ considered in this work can be easily constructed by multiplying the Gaussian exponentials by the appropriate Cartesian spherical harmonics [16,17].

With the general form of the ECG matrix-elements algorithms and with efficient parallelisation of the computer code for use on massively parallel systems, the main bottleneck limiting the size of the atomic systems which can be calculated with these types of all-electron Gaussian functions is the *n*! dependence of the computational time on the number of the electron in the atom. Thus very accurate calculations can, at present, be performed for atoms with no more than five electrons [2-5]. Even though we wrote and implemented codes to perform ECG calculations for bound states of atoms with six and seven electrons, e.g. the carbon and nitrogen atoms, [18,19], the computational resources available to us at the present time to carry out high-accuracy atomic calculations do not permit consideration of atoms with more than five electrons.

As the internal nonrelativistic Hamiltonian explicitly depends on the mass of the nucleus, the present

calculations are performed for the stable beryllium isotope which is ⁹Be. Calculations are also done for the beryllium atom with an infinite mass, ${}^{\infty}$ Be. The present calculations include the leading spin-independent relativistic corrections. The algorithms for calculating these corrections for D states were recently implemented [17]. The algorithms are expressed in terms of the internal coordinates and some of them explicitly depend on the nuclear mass. Also, as the relativistic corrections are calculated as expectation values of the operators representing the relativistic corrections with nonrelativistic wave function, which is slightly different for ${}^9\mathrm{Be}$ and ${}^\infty\mathrm{Be}$, an additional dependency on the nuclear mass appears in the calculation of the relativistic effects. This dependency is usually called a recoil effect, i.e. the relativistic effect associated with the motion of the nucleus around the centre of mass of the atom.

2. The method

In the present calculations, the internal coordinates, \mathbf{r}_i , i = 1, ..., n, where n is the number of electrons, are Cartesian coordinates of the vectors with the origins at the nucleus and with the ends at the different electrons. In this internal coordinate system, the internal Hamiltonian is expressed as follows [20]:

$$\hat{\mathbf{H}} = -\frac{1}{2} \left(\sum_{i=1}^{n} \frac{1}{\mu_i} \nabla_{\mathbf{r}_i}^T \cdot \nabla_{\mathbf{r}_i} + \frac{1}{m_0} \sum_{\substack{i,j=1\\i \neq j}}^{n} \nabla_{\mathbf{r}_i}^T \cdot \nabla_{\mathbf{r}_j} \right) + \sum_{i=1}^{n} \frac{q_0 q_i}{r_i} + \sum_{i>j=1}^{n} \frac{q_i q_j}{r_{ij}},$$
(1)

where m_0 is the mass of the nucleus and q_0 is its charge, q_i are the electron charges $(q_i = -1)$, and $\mu_i = m_0 m_i / (m_0 + m_i)$ is the reduce mass of electron $i \ (m_i, i = 1, ..., n, are the electron masses). T in (1)$ denotes the matrix/vector transposition. As one can see, the internal Hamiltonian is invariant upon rotations with respect to the centre of the internal coordinate system and represents the motion of n particles, whose charges are the electron charges and the masses are the reduced electron masses, in the central field of the nuclear charge. These particles we call 'pseudo-electrons'. The approach used in separating out the centre-od-mass motion and in deriving the internal Hamiltonian is analogical to the standard textbook approach used to solve the Schrödinger equation for the hydrogen atom.

The ECGs used in the present work to expand the special part of the wave function for the 3D $M_L = 0$ states of beryllium atom considered in the present work is expanded in terms of the basis functions being the following products of Gaussian exponentials and Cartesian angular harmonics:

$$\phi_k^{(L=2)} = (x_{i_k} x_{j_k} + y_{j_k} y_{i_k} - 2z_{i_k} z_{j_k})$$

$$\times \exp \left[-\mathbf{r}^T (A_k \otimes I_3) \mathbf{r} \right], \tag{2}$$

where electron labels i_k and j_k can vary from 1 to n (n = 4for the neutral beryllium atom), with $i_k \ge j_k$ and with i_k and j_k either equal or not equal to each other. The $i_k \ge j_k$ case can be called a 'p² configuration'. and the $i_k = j_k$ case can be called an 'sd configuration'. In (2), A_k is an $n \times n$ symmetric matrix of the real exponential parameters, which is unique to each ECG, ⊗ denotes the Kronecker product, I_3 is an 3×3 identity matrix, and \mathbf{r} is the following 3n vector of the internal Cartesian coordinates:

$$\mathbf{r} = \begin{pmatrix} \mathbf{r}_1 \\ \mathbf{r}_2 \\ \vdots \\ \mathbf{r}_n \end{pmatrix} = \begin{pmatrix} x_1 \\ y_1 \\ z_1 \\ \vdots \\ x_n \\ y_n \\ z_n \end{pmatrix}. \tag{3}$$

 $(A_k \otimes I_3)$ is denoted as \mathbf{A}_k .

 \mathbf{A}_k has to be positive definite to Gaussian (2) be square integrable. To make A_k be positive definite we represent it in the following Cholesky-factored form: $\mathbf{A}_k = (L_k L_k^T) \otimes I_3$, where L_k is an $n \times n$ lower-triangular matrix of real numbers. Being in that form, A_k is automatically positive definite for the L_k matrix elements being any real numbers. It is convenient to use the L_k matrix elements and not the A_k matrix elements as the variationally adjusted parameters in the calculation because they can be optimised in an unrestricted range of values from $-\infty$ to $+\infty$. If the A_k matrix elements were chosen as the variational parameters, their optimisation would be constrained by the condition that the A_k matrix must be positive definite. A constrained optimisation is usually more cumbersome than an unconstrained

The present calculations concern states with the triplet multiplicity. In constructing the wave function, one needs to impose proper permutational symmetry. In the present work, this is done using the so-called spin-free formalism [21-23], which involves the construction of an appropriate symmetry projector, P, that by acting on a basis function makes it comply with the desired permutational-symmetry properties. In the present work, P is generated using the appropriate Young operator which is constructed for the triplet state of the four-electron beryllium atom [21-23]. The procedure for constructing Young operators in ECG calculations was described in our earlier work [24]. For the presently considered 3D states the P operator is:

$$P = (1 + P_{12})(1 - P_{14} - P_{34})(1 - P_{13}), (4)$$

where P_{ii} permutes the spatial internal coordinates of the ith and jth pseudo-electrons.

The internal Hamiltonian (1), as well as the operators representing the leading relativistic corrections (see the next section), are symmetric with respect to any permutation of the labels of the pseudo-electrons. Thus, in calculating the Hamiltonian, overlap, and the energygradient matrix elements, as well as the matrix elements for the operators representing the relativistic corrections, the symmetry operator, P, can be moved from the bra side of the integral to the *ket* side. Thus symmetry operator $P^{\dagger}P$ appears on the ket side of the integral. That operator has 4! = 24 terms which makes each matrix element to be a linear combination of 24 primitive spatial integrals and the whole calculation to scale as 4!. The algorithms for calculating the Hamiltonian, overlap, energy-gradient matrix elements, with ECGs (2), were presented in Ref. [16].

2.1. Relativistic operators

In the present work, we consider the relativistic corrections that do not result in fine/hyperfine splitting of the energy levels obtained in the non-relativistic variational calculations. These corrections are of the order of α^2 , where α is the fine-structure constant ($\alpha = \frac{1}{c}$, where c is the speed of light in the atomic units). They represent the mass-velocity (MV), Darwin (D), orbit-orbit (OO) and spin-spin Fermi contact (SS) relativistic effects. The spin-orbit interaction, that for ³D states results in splitting the energy levels into lines corresponding to J =1, 2, and 3, are not included in the present calculations. The MV, D, OO and SS operators have the following form in terms of the internal coordinates: *mass-velocity term*:

$$\hat{H}_{\text{MV}} = -\frac{1}{8} \left[\frac{1}{m_0^3} \left(\sum_{i=1}^n \nabla_{\mathbf{r}_i} \right)^4 + \sum_{i=1}^n \frac{1}{m_i^3} \nabla_{\mathbf{r}_i}^4 \right]$$
 (5)

Darwin term:

$$\hat{H}_{D} = \frac{\pi}{2} \sum_{i=1}^{n} \left(\frac{4}{3} \frac{1}{m_{0}^{2}} + \frac{1}{m_{i}^{2}} \right) q_{0} q_{i} \delta^{3}(\mathbf{r}_{i})$$

$$+ \frac{\pi}{2} \sum_{i=1}^{n} \sum_{i\neq i}^{n} \frac{1}{m_{i}^{n}} q_{i} q_{j} \delta^{3}(\mathbf{r}_{ij})$$
(6)

orbit-orbit term:

$$\hat{H}_{OO} = -\frac{1}{2} \sum_{i=1}^{n} \sum_{j=1}^{n} \frac{q_0 q_j}{m_0 m_j}$$

$$\times \left[\frac{1}{r_j} \nabla_{\mathbf{r}_i}^T \cdot \nabla_{\mathbf{r}_j} + \frac{1}{r_j^3} \mathbf{r}_j^T \cdot (\mathbf{r}_j^T \cdot \nabla_{\mathbf{r}_i}) \nabla_{\mathbf{r}_j} \right]$$

$$+ \frac{1}{2} \sum_{i=1}^{n} \sum_{j>i}^{n} \frac{q_i q_j}{m_i m_j}$$

$$\times \left[\frac{1}{r_{ij}} \nabla_{\mathbf{r}_i}^T \cdot \nabla_{\mathbf{r}_j} + \frac{1}{r_{ij}^3} \mathbf{r}_{ij}^T \cdot (\mathbf{r}_{ij}^T \cdot \nabla_{\mathbf{r}_i}) \nabla_{\mathbf{r}_j} \right]$$
(7)

and spin-spin term:

$$H_{SS} = -\frac{8\pi}{3} \sum_{\substack{i,j=1\\i>i}}^{4} \frac{q_i q_j}{m_i m_j} \left(\mathbf{s}_i \cdot \mathbf{s}_j \right) \delta \left(\mathbf{r}_{ij} \right), \tag{8}$$

where $\delta(\mathbf{r})$ is the Dirac delta function, $\nabla_{\mathbf{r}_i}$ is the nabla operator acting on the coordinates of vector \mathbf{r}_i , and \mathbf{s}_i is the spin operator for electron i. For the ${}^{3}D$ states considered in this work,

$$\left\langle \sum_{\substack{i,j=1\\i>i}}^{4} \left(\mathbf{s}_{i} \cdot \mathbf{s}_{j} \right) \delta \left(\mathbf{r}_{ij} \right) \right\rangle = -\frac{3}{4} \left\langle \sum_{\substack{i,j=1\\i>i}}^{4} \delta \left(\mathbf{r}_{ij} \right) \right\rangle. \tag{9}$$

The explicit formulas for calculating the matrix elements of the above relativistic operators were derived in our previous paper [17].

2.2. The calculations

The computer double precision is used in the present calculations. The code performing the nonrelativistic calculation for a particular state and the optimisation of the exponential non-linear parameters of the Gaussians in written in Fortran 90 and involves MPI (message passing interface) parallelisation. For each considered state the ECG basis functions are independently optimised.

In the first step of the calculations, the nonrelativistic energies and the corresponding wave functions are determined for the lowest four ¹D states of ⁹Be. For each state, the basis set is grown to the size of 15,300 functions. The growing procedure involves multiple steps with each of them consisting of adding a certain number of functions one by one and optimising them using a procedure that employs the analytically derived energy-gradient vector. To generate the initial parameters of a newly added Gaussian, the parameters of the Gaussians already include in the basis set are perturbed using a procedure that employs a random number generator. The perturbed function that lowers to the energy the most is used as the initial guess in the optimisation. However, before the optimisation is performed, the i_k and j_k pseudo-electron indices of the optimised ECG (see (2)) are optimised. More details of the procedure used in growing the ECG basis set can be found in our previous paper [17].

The use of the one-function-at-a-time approach in growing the basis set and in optimising the added functions allows to monitor and eliminate any lineardependency between the ECGs that may appear in the calculation. An appearance of linear dependency among the basis functions is undesirable because it may cause numerical instabilities and loss of accuracy in the calculation. To determine the linear expansion coefficients of the ECGs in the wave function, the standard procedure for solve the secular equation problem is employed.

After the 15,300-ECGs basis sets are generated for the four lowest ³D states of ⁹Be, they are used to calculated the energies and the corresponding wave functions of [∞]Be. No reoptimisation of the Gaussian non-linear parameters is performed. Only the linear expansion coefficients are reoptimised by solving the secular problem with the Hamiltonian matrix calculated with the internal Hamiltonian where the ⁹Be nuclear mass is replaced with an infinite mass. Such an approach usually works quite well for lower Rydberg atomic states [16]. The reoptimisation of the expansion coefficient usually suffices to account for the change of the wave function and the energy due to the change of the nuclear mass [17].

In the final step, the nonrelativistic wave functions obtained for the lowest four 3D states of ${}^9\mathrm{Be}$ and ${}^\infty\mathrm{Be}$ are used to calculate the relativistic corrections. Then these corrections are added to the nonrelativistic energies to calculate the total energies. The total energies are then used to calculate the transition energies with respect to the beryllium ¹*S* ground state.

3. Results

The results of the variational calculations concerning growing of the ECG basis sets for the four lowest 1s²2snd, n = 3, 4, 5, and 6, states of ⁹Be are presented in Table 1. The energy values corresponding the basis set of 12,600, 13,500, 14,400 and 15,300 are shown in the table to assess the convergence of the basis growing process. As one can see, for all considered states, the ninth significant figure after the decimal point in each energy value is virtually converged. As expected, the convergence level is marginally lower for the fourth state than for the lower states. There seems to be no need to increase the basis set size any further.

The largest basis set of 15,300 ECGs for each state is used to calculate the total nonrelativistic energy for ${}^{\infty}$ Be.

Table 1. Convergence of the nonrelativistic energies, E_{nrel} , of the four lowest ³D states of ⁹Be with the number of the ECG basis functions.

State	Basis	E_{nrel}
1s ² 2s3d	12600	-14.383731176
	13500	-14.383731178
	14400	-14.383731180
	15300	-14.383731181
1s ² 2s4d	12600	-14.356902134
	13500	-14.356902137
	14400	-14.356902140
	15300	-14.356902142
1s ² 2s5d	12600	-14.344772363
	13500	-14.344772368
	14400	-14.344772372
	15300	-14.344772376
1s ² 2s6d	12600	-14.338275846
	13500	-14.338275856
	14400	-14.338275864
	15300	-14.338275872

Note: The energies are given in hartrees.

Table 2. Nonrelativistic energies of the four lowest ³D states of 9 Be and $^\infty$ Be calculated with 15,300 ECG base functions.

State	⁹ Be	∞Be
1s ² 2s3d	-14.383731181	-14.384634628
1s ² 2s4d	-14.356902142	-14.357803959
1s ² 2s5d	-14.344772376	-14.345673406
1s ² 2s6d	-14.338275872	-14.339176478

Note: The energies are given in hartrees.

The results are shown in Table 2. As expected, making the nuclear mass heavier lowers the total energy. The lowering is about 0.001 hartree and decreases slightly as the level of excitation decreases. This effect is due to an increase of the reduced mass of the electron caused by the increase of the nuclear mass. As a result, the electrons are slightly closer to the nucleus in $^{\infty}$ Be than in ⁹Be. This makes the total energy of $^{\infty}$ Be being lower than the energy of ⁹Be. However, the lowering of the energies of the four electrons due to the increasing nuclear mass is somewhat uneven. Particularly, the energy of the Rydberg d electron is lowered more for the lowest state, where it is located closer to the nucleus, than for the fourth state. The total energies calculated for ⁹Be and [∞]Be and shown in Table 2 may provide a reference for future nonrelativistic calculations performed by other researchers for an infinite nuclear mass (i.e. with assuming the Born-Oppenheimer approximation).

The $^{\infty}$ Be nonrelativistic energy for the lowest ^{3}D state obtained in this work can be compared with the energy recently calculated by Puchalski et al. [25] They also used ECGs in their calculations and their largest basis set generated for the lowest 3D state consisted of 8192 functions. For that basis set their $^{\infty}$ Be energy was -14.38463460377 hartree (their extrapolated their energies to an infinite basis set and

Table 3. The non-relativistic energies, E_{nrel} , and α^2 mass-velocity (MV), Darwin (D), orbit-orbit (OO) and spin-spin (SS) α^2 relativistic energy corrections for the 1s²2snd, n = 3, 4, 5, and 6, ³D states of ⁹Be and ∞ Be.

Isotope	Basis	E_{nrel}	$E_{\rm MV} \times 10^2$	$E_{\rm D} \times 10^2$	$E_{00} \times 10^{-1}$	E_{SS}	$\alpha^2 \Delta E_{\rm rel} \times 10^{-3}$
			Sta	ite 1s ² 2s3d			
⁹ Be	6000	-14.383731105	-2.680289	2.154023	-9.318846	9.888997	-2.325461
	6900	-14.383731131	-2.680367	2.154098	-9.318842	9.888939	-2.325475
	7800	-14.383731147	-2.680370	2.154102	-9.318843	9.888604	-2.325487
$^{\infty}$ Be	7800	-14.384634593	-2.681031	2.154500	-9.055109	9.890245	-2.325400
			Sta	ite 1s ² 2s4d			
⁹ Be	6000	-14.356902021	-2.681450	2.154782	-9.348216	9.915980	-2.326320
	6900	-14.356902066	-2.681465	2.154819	-9.348217	9.915953	-2.326201
	7800	-14.356902090	-2.681644	2.154966	-9.348218	9.915850	-2.326377
$^{\infty}$ Be	7800	-14.357803907	-2.682306	2.155364	-9.084342	9.917496	-2.326290
			Sta	ite 1s ² 2s5d			
⁹ Be	6000	-14.344772185	-2.681576	2.154824	-9.356135	9.924896	-2.326335
	6900	-14.344772254	-2.681749	2.154987	-9.356137	9.924827	-2.326392
	7800	-14.344772291	-2.681866	2.155000	-9.356138	9.924732	-2.326419
$^{\infty}$ Be	7800	-14.345673321	-2.682528	2.155497	-9.092218	9.926380	-2.326332
			Sta	ite 1s ² 2s6d			
⁹ Be	6000	-14.338275518	-2.681527	2.154713	-9.359207	9.928281	-2.326498
	6900	-14.338275636	-2.681824	2.154986	-9.359210	9.927988	-2.326644
	7800	-14.338275705	-2.681946	2.155094	-9.359215	9.927960	-2.326718
∞Be	7800	-14.339176310	-2.682608	2.155492	-9.095274	9.929609	-2.326630

Note: The convergence of the results in terms of the number of ECGs for ⁹Be is shown. All values are given in hartrees.

Table 4. Transition energies calculated for the four lowest ³D $1s^2 2snd$, n = 3, 4, 5, and 6 states of $^9 Be$ and $^\infty Be$ with respect to the ground 1s²2s² ¹S state.

Isotope	ΔE_{nrel}	ΔE_{rel}	NIST
		State 1s ² 2s3d	
⁹ Be	62 046.4320	62 054.0711	62 053.740 \pm 0.06
$^{\infty}$ Be	62 050.2806	62 057.9509	
		State 1s ² 2s4d	
⁹ Be	67 934.7254	67 942.1691	$67\ 941.65\pm0.08$
$^{\infty}$ Be	67 938.9316	67 946.4065	
		State 1s ² 2s5d	
⁹ Be	70 596.9014	70 604.3358	70 603.74 \pm 0.06
$^{\infty}$ Be	70 601.2803	70 608.7461	
		State 1s ² 2s6d	
⁹ Be	72 022.7192	72 030.0882	72 029.50 \pm 0.08
$^{\infty}$ Be	72 027.1913	72 034.5916	

Note: The non-relativistic transition energies, ΔE_{nrel} , are calculated for the 3D states using 15,300 ECGs. In calculating the transition energies that account for the relativistic corrections, $\Delta E_{\rm rel}$, these corrections for the 3D states are calculated using 7800 ECGs while the nonrelativistic energies are calculated using 15,300 ECGs. All values are given in cm⁻¹. In calculating the transitions energies, the following ground-state energies of ${}^9\text{Be}$ and ${}^\infty\text{Be}$ obtained with 16,000 ECG basis functions are used: $E_{nrel} = -14.666435526$ (9 Be) and $E_{rel} = -14.668795820$ hartree (9 Be), and $E_{nrel} = -14.667356508$ ($^\infty$ Be) and $E_{rel} = -14.669716857$ hartree ($^\infty$ Be) [1]. The transition energies are compared with the experimental results [15]. Each experimental value is obtained as the gravity centre of the corresponding fine-structure multiplet.

obtained -14.3846346167 hartree), while our present result obtained with 15,300 **ECGs** -14.384634628 hartree, which is even lower than their extrapolated value.

The leading MV, D, OO and SS relativistic corrections are calculated for both 9 Be and ${}^{\infty}$ Be. The present version of our computer code for calculating these corrections does not allow for use of large basis sets. Thus the present calculations are performed with basis sets of 6000, 6900 and 7800 ECGs for ⁹Be and with the basis sets of 7800 ECGs for $^{\infty}$ Be. The results are shown in Table 3. Upon

examining the results one can notice that the convergence of the total relativistic correction for each of the four state of ⁹Be is similar to the convergence of the total nonrelativistic energy particularly for the lowest states. It is interesting that the recoil effect, which can be calculated for each state as a difference between the total relativistic corrections corresponding to 9 Be and ${}^{\infty}$ Be is remarkably similar for all four states. It raises the value of the relativistic correction by 0.000087×10^{-3} hartree for states $1s^2 2$ snd, n = 3, 4, and 5, and by 0.0000088×10^{-3} hartree for the 1s²2s6d state.

Finally, the total nonrelativistic energies of ⁹Be and $^{\infty}$ Be calculated with 15,300 ECGs and the corresponding total energies obtained by adding the relativistic corrections calculated with 7800 ECGs to the nonrelativistic energies calculated with 15,300 ECGs are used to calculate the interstate transition energies with respect to the ¹S ground state of beryllium. The ¹S ground-state energies of ${}^9\mathrm{Be}$ and ${}^\infty\mathrm{Be}$ are taken from our recent paper [1] where they were calculated using 16,000 ECGs. The interstate transition energies calculated for ${}^9\text{Be}$ and ${}^\infty\text{Be}$ with and without the relativistic corrections are presented in Table 4 where they are compared with the experimental results taken from Ref. [14,15]. Upon examining the results in Table 4 one can make the following observations. The contribution from the relativistic corrections to the transition energy of each of the four states is about $+8 \,\mathrm{cm}^{-1}$ and the contribution from the finitemass effect is about -4 cm^{-1} . The differences between the transition energies calculated for ⁹Be using the energies that include the relativistic corrections with the experimental results is smaller than about 0.6 cm⁻¹ (0.331, $0.519, 0.596, \text{ and } 0.60 \text{ cm}^{-1} \text{ for states } 1\text{s}^22\text{snd}, n = 3, 4, 5,$



and 6, respectively). For the experimental values used for the comparison in Table 4 we use the 'gravity centre' of the fine-structure multiplet for each energy level.

4. Summary

In summary, transition energies between the four lowest ³D Rydberg states and the ¹S ground state of the beryllium atom are calculated using the finite-nuclear-mass approach that includes the leading spin-independent relativistic corrections. Large basis sets of all-electron explicitly correlated Gaussian functions are used in the calculations of the 3D states. The transition energies agree with the experimental values to within about $0.6 \,\mathrm{cm}^{-1}$. Including the leading quantum electrodynamics (QED) effects would likely improve the agreement between the calculated values and the experiment. This was recently demonstrated in the calculations performed by Puchalski et al. [25] where the lowest beryllium ³D state was considered. Also, it would be interesting to calculate the fine and hyperfine structure of the ³D levels. Algorithms for calculating the spin-orbit interactions contributing to the fine splitting of ${}^{3}D$ levels of atoms are currently being developed in our lab.

Acknowledgments

We dedicate this work to the memory of Professor Lutosław Wolniewicz. Throughout many years, he had been very supportive and helpful in our work. On numerous occasions he had shared with us his unpublished results and offered useful comments concerning our research.

Disclosure statement

No potential conflict of interest was reported by the author(s).

Funding

This work has also been supported by a grant from the National Science Foundation; grant no. 1856702. L. A. also acknowledges the support of the Centre for Advanced Study (CAS), the Norwegian Academy of Science and Letters, in Oslo, Norway, which funds and hosts our research project titled: Attosecond Quantum Dynamics Beyond the Born-Oppenheimer Approximation, during the 2021-22 academic year. The authors are grateful to the University of Arizona Research Computing for providing computational resources for this work.

References

[1] S. Nasiri, L. Adamowicz and S. Bubin, J. Phys. Chem. Ref. Data 50, 043107 (2021). doi:10.1063/5.0065282

- [2] M. Stanke, D. Kedziera, S. Bubin and L. Adamowicz, Phys. Rev. Lett. 99, 043001 (2007). doi:10.1103/PhysRevLett.99. 043001
- [3] S. Bubin, J. Komasa, M. Stanke and L. Adamowicz, Phys. Rev. A 81, 052504 (2010). doi:10.1103/PhysRevA.81. 052504
- [4] S. Bubin, J. Komasa, M. Stanke and L. Adamowicz, J. Chem. Phys. 132, 114109 (2010). doi:10.1063/1.3358
- [5] S. Bubin, M. Stanke and L. Adamowicz, J. Chem. Phys. 131, 044128 (2009). doi:10.1063/1.3195061
- [6] M. Puchalski, J. Komasa and K. Pachucki, Phys. Rev. A 87, 030502(R) (2013). doi:10.1103/PhysRevA.87.030
- [7] M. Stanke, J. Komasa, S. Bubin and L. Adamowicz, Phys. Rev. A 80, 022514 (2009). doi:10.1103/PhysRevA.80. 022514
- [8] I. Hornyák, L. Adamowicz and S. Bubin, Phys. Rev. A 100, 032504 (2019). doi:10.1103/PhysRevA.100.032504
- [9] E.C. Cook, A.D. Vira, C. Patterson, E. Livernois and W.D. Williams, Phys. Rev. Lett. 121, 053001 (2018). doi:10.1103/PhysRevLett.121.053001
- [10] K.L. Sharkey, S. Bubin and L. Adamowicz, Phys. Rev. A 84, 044503 (2011). doi:10.1103/PhysRevA.84.044
- [11] M. Stanke, E. Palikot, K.L. Sharkey and L. Adamowicz, Chem. Phys. Lett. 779, 138823 (2021). doi:10.1016/j. cplett.2021.138823
- [12] W.R. Bozman, C.H. Corliss, W.F. Meggers and R.E. Trees, J. Res. Natl. Bur. Stand. 50, 131 (1953). doi:10.6028/jres. 050.020
- [13] L. Johansson, Ark. Fys. 23, 119 (1963).
- [14] A. Kramida and W.C. Martin, J. Phys. Chem. Ref. Data 26, 1185 (1997), doi:10.1063/1.555999
- [15] A. Kramida, Yu. Ralchenko, J. Reader, NIST ASD Team, NIST Atomic Spectra Database (Version 5.7.1) (National Institute of Standards and Technology, Gaithersburg, 2019). https://physics.nist.gov/asd.
- [16] K.L. Sharkey, S. Bubin and L. Adamowicz, J. Chem. Phys. 134, 044120 (2011). doi:10.1063/1.3523348
- [17] M. Stanke and L. Adamowicz, Phys. Rev. A 100, 042503 (2019). doi:10.1103/PhysRevA.100.042503
- [18] K.L. Sharkey, M. Pavanello, S. Bubin and L. Adamowicz, Phys. Rev. A 80, 062510 (2009). doi:10.1103/PhysRevA. 80.062510
- [19] K.L. Sharkey and L. Adamowicz, J. Chem. Phys. 140, 174112 (2014). doi:10.1063/1.4873916
- D.B. Kinghorn and R.D. Poshusta, Phys. Rev. A 47, 3671 (1993). doi:10.1103/PhysRevA.47.3671
- [21] F.A. Matsen and R. Pauncz, The Unitary Group in Quantum Chemistry (Elsevier, Amsterdam, 1986).
- [22] R. Pauncz, Spin Eigenfunctions (Plenum, New York, 1979).
- [23] M. Hamermesh, Group Theory and Its Application to Physical Problems (Addison-Wesley, Reading, MA,
- [24] S. Bubin, M. Cafiero and L. Adamowicz, Adv. Chem. Phys. 131, 377 (2005). doi:10.1002/0471739464.ch6
- [25] M. Puchalski, J. Komasa and K. Puchacki, Phys. Rev. A **104**, 022824 (2021). doi:10.1103/PhysRevA.104.022824